Article



Study of the Expression Transition of Cardiac Myosin Using Polarization-Dependent SHG Microscopy

Cai Yuan, ¹ Xiaolei Zhao, ² Zhonghai Wang, ¹ Thomas K. Borg, ³ Tong Ye, ¹ Zain I. Khalpey, ⁴ Raymond B. Runyan, ⁵ Yonghong Shao, ^{6,*} and Bruce Z. Gao^{1,*}

¹Departments of Bioengineering and ²Electrical and Computer Engineering, Clemson University, Clemson, South Carolina; ³Department of Regenerative Medicine and Cell Biology, Medical University of South Carolina Charleston, South Carolina; ⁴Departments of Surgery and ⁵Cellular and Molecular Medicine, University of Arizona, Tucson, Arizona; and ⁶College of Optoelectronics Engineering, Shenzhen University, Shenzhen. China

ABSTRACT Detection of the transition between the two myosin isoforms α - and β -myosin in living cardiomyocytes is essential for understanding cardiac physiology and pathology. In this study, the differences in symmetry of polarization spectra obtained from α - and β -myosin in various mammalian ventricles and propylthiouracil-treated rats are explored through polarization-dependent second harmonic generation microscopy. Here, we report for the, to our knowledge, first time that α - and β -myosin, as protein crystals, possess different symmetries: the former has C6 symmetry, and the latter has C3v. A single-sarcomere line scan further demonstrated that the differences in polarization-spectrum symmetry between α - and β -myosin came from their head regions: the head and neck domains of α - and β -myosin account for the differences in symmetry. In addition, the dynamic transition of the polarization spectrum from C6 to C3v line profile was observed in a cell culture in which norepinephrine induced an α - to β -myosin transition.

SIGNIFICANCE Although the transition from α - to β -myosin expression is prevalent in diseased mammalian myocardia (e.g., cardiac hypertrophy), current methods of quantitatively studying myosin isoform transition are not only inefficient, they are useless at detection in vivo. Here, we show for the, to our knowledge, first time that crystal structures around the myosin head regions of α - and β -myosin differ and can be dynamically detected in living tissue via polarization-dependent second harmonic generation microscopy. Our finding provides a new method for basic research on the dynamic recognition of α - and β -myosin.

INTRODUCTION

In mammalian myocardia, two closely related myosin isoforms, α - and β -myosin, are expressed. The differential expression of these myosin isoforms is important in regulation of cardiac contractile performance (1). α -myosin is responsible for greater actin-activated ATPase activity and thus fast actin-filament sliding velocity. The actin-activated ATPase activity and actin-filament sliding velocity of β -myosin are two to three times lower (2). Mammalian species express different ratios of α -/ β -myosin depending on developmental and pathophysiologic conditions during car-

 $Submitted\,August\,9,\,2019,\,and\,accepted\,for\,publication\,December\,27,\,2019.$

*Correspondence: shaoyh@szu.edu.cn or zgao@clemson.edu

Editor: David Warshaw.

https://doi.org/10.1016/j.bpj.2019.12.030

© 2019

diac remodeling (3). Studies indicate that a small change in the myosin isoform ratio significantly alters cardiac function (4,5). Myosin isoform transition in mammalian myocardia is closely associated with abnormal hormone secretion (6), increased mechanical load (7–9), and other heart diseases. For example, healthy human heart ventricles express myosin isoforms with an α/β ratio of \sim 1:9, whereas failing human ventricles express no detectable α -myosin (2,10,11). The percentage of α -myosin is linearly reduced in enlarged atria when indexed to the left atrial transverse diameter (12). Reportedly, chronic alcohol intake can significantly change the myosin composition of mammalian myocardia (13).

Study of the transition between myosin isoforms during heart remodeling is critical to understanding heart physiology and pathology. However, although functionally distinct, the two myosin isoforms show considerable



homology. For example, 95% of their amino acids are identical (14,15), and the difference in their molecular mass is less than 0.2% (14,16,17). Conventional methods of distinguishing these myosin isoforms, such as Western blotting, are not only inefficient but also inapplicable to living tissue and thus cannot be used to study the dynamic transition between the two myosin isoforms in a living cardiomyocyte (17-19).

Second harmonic generation (SHG) microscopy has been widely applied for visualizing noncentrosymmetric biomolecules in living tissues (e.g., myosin and collagen) without labeling (20). Polarization-dependent SHG (P-SHG) microscopy can explore the crystallographic structure of biomolecules. Cardiac sarcomeric myosin was conventionally known to possess hexagonal and/or cylindrical symmetry (class C6) in nonlinear optics (21–23). Our experimental results showed that the polarization spectra of this type of myosin had a C6 line profile in the myocardia of small mammals such as rat and mouse. The myosin with C3v-line-profiled polarization spectra dominated in large mammals such as pig and human. This may be due to a species dependence of the expression of myosin isoform because α -myosin dominates in small mammalian myocardia, whereas β -myosin dominates in large mammalian myocardia. Therefore, we hypothesized that these myosin isoforms possessed different crystal symmetry, and this crystallographic difference could be captured by P-SHG microscopy.

In this work, we used the hypothyroidism drug propylthiouracil (PTU) to induce the transition of cardiac myosin expression from the α - to the β -isoform in rat myocardia. We observed a shift in the crystal symmetry of the cardiac myosin from C6 to C3v based on the SHG polarization spectra during this transition. The percentage of C3v-lineprofiled polarization spectra was linearly correlated to the percentage of β -myosin. Further, in cell-culture experiments, cardiomyocytes were treated with the adrenergic agent norepinephrine (NE) to induce myosin transition from α - to β -isoforms. In our final experiments, the timedependent transition of the polarization spectrum from C6 to C3v symmetry was observed in a single cardiomyocyte. Through scanning myosin filaments in a single sarcomere, we found that transition of the polarization spectrum from C6 to C3v line profiles occurred in the regions where cross-bridges are formed. Our study may pave the way for the α - and β -myosin discrimination and diagnosis of related diseases, such as cardiac hypertrophy, at the cellular and molecular levels.

METHODS AND MATERIALS

SHG of C6- and C3v-symmetric crystal

Under an excitation light with an angular frequency of ω , the induced second-order nonlinear polarization density P at frequency 2ω can be described as

$$P_i^2(2\omega) = \sum_{jk} \chi_{ijk}^2(\omega, \omega) E_j(\omega) E_k(\omega) \qquad i, j, k = 1, 2, 3,$$
(1)

where χ^2_{ijk} is the second-order nonlinear susceptibility tensor (second-NST) with 27 $(3 \times 3 \times 3)$ components. In the case of SHG, the second-NST components χ^2_{iik} can be represented as a 3 \times 6 matrix d. Myosin is generally considered to possess cylindrical symmetry (class C6), which has been confirmed by a great number of studies on myosin in small mammalian myocardia (21–23). Its d matrix is given by:

$$d_{c6} = \left[egin{array}{ccccc} 0 & 0 & 0 & d_{15} & 0 & 0 \ 0 & 0 & 0 & d_{15} & 0 & 0 \ d_{31} & d_{31} & d_{33} & 0 & 0 & 0 \end{array}
ight],$$

where d_{15} , d_{31} , and d_{33} are the only nonzero components. Fig. 1 A shows the coordinate system that we defined to describe the orientation of the myofibril and the excitation light polarization. It is assumed that the myofibril is located on the y-z plane and oriented along the z axis. The excitation light is incident along the x axis, with electric field polarization on the y-z plane. α is denoted the angle between the incident polarization and the z axis. The three electric field components can be expressed as $E_v(\omega) = E \sin \alpha$, $E_z(\omega) = E \cos \alpha$, and $E_x(\omega)$ is ~ 0 . Thus, based on the d matrix, the relationship between the intensity of the emitted SHG and the angle α is described as

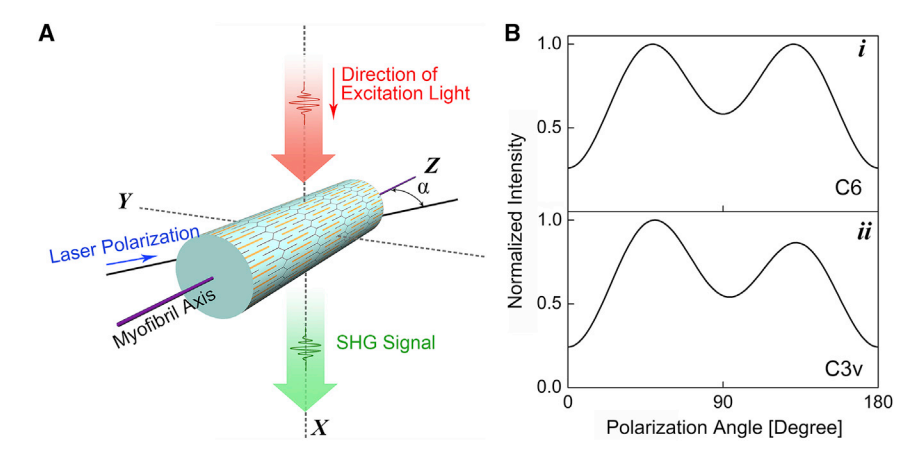


FIGURE 1 (A) Geometric arrangement of a single myofibril relative to the polarization of the applied excitation light. α : angle between the incident polarization of the excitation light and the zaxis of the myofibril. (B) Simulated plots of normalized SHG intensity as a function of polarization angle for myosin are shown: (i) cylindrical C6 and (ii) trigonal C3v crystal class symmetry (polarization spectrum describes the relationship between the normalized intensity of the SHG signal and the polarization angle α of the excitation light). The normalization is performed by dividing the 18 values collected in different polarization states by the maximal one such that the maximal value in the normalized polarization spectrum is equal to 1. To see this figure in color, go online.

Yuan et al.

$$I_{c6}^{2\omega} \sim \left[(\sin 2\alpha)^2 + \left(\frac{d_{31}}{d_{15}} \sin^2 \alpha + \frac{d_{33}}{d_{15}} \cos^2 \alpha \right)^2 \right].$$
 (2)

However, our data showed that in the myocardia of large mammals, most of the myosin exhibits trigonal symmetry (class C3v). For C3v symmetry, the d matrix is given by (24,25)

$$d_{c3v} = \begin{bmatrix} 0 & 0 & 0 & d_{15} & 0 & -d_{22} \\ -d_{22} & d_{22} & 0 & d_{15} & 0 & 0 \\ d_{31} & d_{31} & d_{33} & 0 & 0 & 0 \end{bmatrix},$$

where d_{15} , d_{22} , d_{31} , and d_{33} are the only nonzero components. Similarly, the relationship between the intensity of the emitted SHG and the polarization angle of the excitation light field is described as

$$I_{c3v}^{2\omega} \sim \left[\left(\frac{d_{22}}{d_{15}} \sin^2 \alpha + \sin 2\alpha \right)^2 + \left(\frac{d_{31}}{d_{15}} \sin^2 \alpha + \frac{d_{33}}{d_{15}} \cos^2 \alpha \right)^2 \right]. \tag{3}$$

To visually demonstrate the difference between C6 and C3v symmetry based on the d matrix, the polarization spectra (the curve of the SHG intensity versus the polarization angle of the incident light) for C6 and C3v symmetry are plotted in Fig. 1 B (the settings are $d_{31}/d_{15} = 1.00$, $d_{33}/d_{15} = 0.67$, and $d_{22}/d_{15} = 0$ and 0.10, respectively, for C6 and C3v). Fig. 1 Bi shows the polarization spectrum for C6 symmetry ($d_{22} = 0$), where the curve is symmetrical with respect to 90° . A nonzero d_{22} produces the pattern in Fig. 1 Bii, which exhibits noticeable asymmetry with respect to 90°.

The polarization spectrum can be determined experimentally, and the ratio values of the second-NST components $(d_{31}/d_{15}, d_{33}/d_{15}, \text{ and } d_{22}/d_{15})$ can be retrieved by fitting the polarization spectrum according to Eq. 3 (note: if the experimental data fit Eq. 2, when they are fitted to Eq. 3, d_{22}/d_{15} will be very close to 0). Therefore, by comparing the values of the second-NST components, we can study the structural and symmetric discrepancy between myosin isoforms or myosin under different pathological conditions.

P-SHG imaging system

The construction of the P-SHG microscope with an on-stage incubator is shown in Fig. 2 A. The excitation light was generated from a Ti:Sapphire laser (100 fs and 80 MHz, Tsunami 3960-X1BB pumped by a 9.5 W Millennia; Spectra-Physics, Santa Clara, CA) and was tuned to 830 nm. The beam was then steered onto the XY scanner (6210H; Cambridge Technology, Bedford, MA). Before the beam was focused onto the sample using a 0.9 NA water immersion objective (60× LUMPlanFLN; Olympus, Tokyo, Japan), it passed a polarization state generator to rotate the polarization angle of the excitation light. The polarization state generator was composed of a polarizer (LPNIRE100-B; ThorLabs, Newton, NJ) and a half-wave plate (WPH05M-830; ThorLabs) that was mounted on a motorized rotator (PRM1Z8; ThorLabs). By rotating the half-wave plate to an angle of ψ relative to the fixed axis of the polarizer, the polarization of the excitation light was rotated to an angle of 2ψ without a change in the intensity of the excitation light. The beam was subsequently focused onto the sample using the water immersion objective (60× LUMPlanFLN; Olympus). After passing the objective, the polarization ellipticity of the excitation light was >50:1. The SHG signals were collected from the forward scattering direction through an Olympus 1.4 NA oil immersion condenser and recorded by a photomultiplier tube (H7422p-40; Hamamatsu, Hamamatsu City, Japan). An IR filter was placed in line before the photomultiplier tube and was used in addition to a 415 \pm 15 nm bandpass filter (FF01-415/ 10-25; Semrock, Rochester, NY). In this study, the scan rate and the pixel dwell time were set to 500 lines/s and 3.2 μ s, respectively, to achieve a twodimensional imaging rate of approximately one frame per second: each frame contained 512 \times 512 pixels with a pixel size of 0.16 μ m. The lateral and axial resolution were experimentally estimated to be 0.47 and 1.26 μ m, respectively (26).

All live-cell imaging was performed in an on-stage incubator, which was composed of an electronically heated aluminum frame with feedback

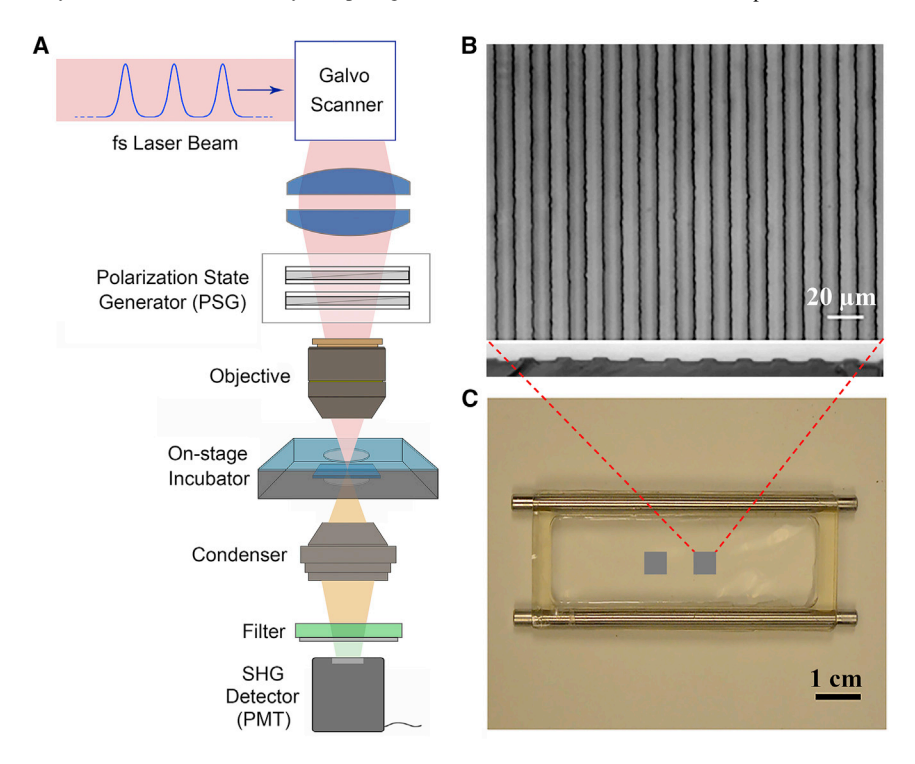


FIGURE 2 (A) Experimental setup of the P-SHG microscope. (B) Grooved PDMS substrate for cardiomyocyte alignment is shown. (C) PDMS culture chamber is shown. Grooved PDMS squares are at the bottom region of this chamber. To see this figure in color, go online.

control and two covers (H301-TC1-HMTC, 2GF-MIXER; Okolab SRL, Ottaviano, Italy). A mixture of 95% air and 5% CO₂ was pumped through the heater unit, which contained deionized water, and the humidified air mixture (~37°C, 95% humidity) was supplied to the chamber of the onstage incubator. The 5% CO2 and 95% humidity mixture was maintained by adjusting the balance between the leakage and the supply through a feedback system. The 37°C temperature inside the culture dish was preserved by adjusting the balance between heat loss and gain through a feedback system, including a temperature sensor placed inside the culture dish.

Sample preparation

In the research reported here, the myocardial samples used for polarizationspectrum-type statistics in different mammalian hearts were from five different mammalian species: four 1-month-old male Sprague Dawley rats, four 1-month-old male CD-1 mice, two 1-month-old female New Zealand White rabbits, and two 3-month-old female Yorkshire White pigs. These heart muscles were provided by Clemson University's animal facility and were harvested from animals used in unassociated studies approved by the Institutional Animal Care and Use Committee of Clemson University. Three human left ventricular samples were obtained from three male heart-transplanted patients of 50-70 years of age. The collection and use of human material were approved by the University of Arizona Institutional Review Board under the CAPTURED protocol.

In the animal experiment that induced myosin isoform transition from α to β , a total of ten 1-month-old Sprague Dawley rats were used (five males and five females, each weighing ~115 g). Four hypothyroid groups were formed; each group had one male and one female randomly selected from the male and female rats, respectively. Animals in each hypothyroid group were administered PTU (500 mg/L; Sigma-Aldrich, St. Louis, MO) in drinking water to induce transition of α - to β -myosin (27,28). PTU administration for each of the four hypothyroid groups lasted for 4, 6, 8, and 10 weeks, respectively, followed by euthanization. The remaining two rats (one male and one female) were used as controls. All procedures were approved by the Clemson University Institutional Animal Care and Use Committee.

The harvested hearts were immediately perfused with cardioplegia high K+ solution to ensure all cardiomyocytes in the muscles were in a relaxed state. The hearts were then fixed by 4% paraformaldehyde perfusion at zero transmural pressure and embedded in optimal cutting temperature compound at -20° C. To avoid variations due to possible regional heterogeneity, all sections were taken from the left ventricle free wall, and sections (\sim 15 μ m) were cut using a cryostat (HM550; Thermo Fisher Scientific, Waltham, MA). The sections were transferred to histology slides. Before the sections were imaged under the P-SHG microscope, the optimal cutting temperature compound was washed away with phosphate-buffered saline, and the sections were secured between glass coverslips.

Cell culture

The cardiomyocytes were isolated and collected as previously described (29). Briefly, 3-day-old Sprague Dawley neonatal rats were euthanized. The hearts were minced into 1 mm³ pieces and first digested with trypsin solution (0.55 mg/mL; Worthington Biochemical, Lakewood, NJ) overnight, then shaken at 75 rpm in a collagenase solution (1 mg/mL collagenase II (Gibco, Gaithersburg, MD) and 0.24 U/mL neutral protease (Worthington Biochemical)) for 1.5 h. The fibroblasts were removed by preincubating the cells in a 150 cm² flask with the normal culture medium (Dulbecco's modified Eagle's medium (DMEM) solution (Thermo Fisher Scientific) and 10% fetal bovine serum (VWR International, Radnor, PA)) for 2 h. The purified cardiomyocyte (~90%) suspension was diluted to 1 million cells/mL and then seeded into grooved polydimethylsiloxane (PDMS) substrate culture dishes coated with fibronectin (20 mg/mL; EMD Millipore, Burlington, MA). The grooved PDMS substrate was used to realize end-to-end cell alignment to mimic in vivo cell morphology (Fig. 2 B). In addition, the four corners of the grooved squares in Fig. 2 C were used to label the locations of the cells.

The isolated neonatal cardiomyocytes were cultured in normal culture medium for 12 h in grooved PDMS substrate. Then, the cells were washed three times with serum-free culture medium (DMEM solution; Thermo Fisher Scientific) and transferred to serum-free medium supplemented with transferrin and insulin (1x; Thermo Fisher Scientific) for 48 h to remove remaining hormones. Then, induction solution was used to induce β -myosin expression (DMEM solution (Thermo Fisher Scientific), 2 μ m/ L NE (Sigma-Aldrich), and 0.1 mM/L vitamin C (Sigma-Aldrich)) (30-32). The NE concentration was maintained for 72 h. In the control group, a DMEM solution containing 0.1 mM/L vitamin C (Sigma-Aldrich) was used. During the 72-h induction period, time-dependent images were taken every 24 h to observe the changes in the P-SHG signal under the effect of the NE.

Image collection and analysis

In this study, images were collected at a 10° interval of the polarization angle of the excitation light, which started from 0° and continued until the polarization angle reached 170°. To eliminate systematic errors such as stage drift, we reversely collected another 18 images with a 10° interval, starting at 170° and returning to the 0° polarization state. An image stack was then formed using the 36 images collected. On the image stack, a region of interest with three to four sarcomeres around a myofibril was randomly selected to calculate the average gray value in each image. To retrieve the ratios of the tensor components, the obtained data were fitted to the model given by Eq. 3 (a nonlinear least-squares method implemented in MATLAB (The MathWorks, Natick, MA) was used, with four parameters as specified: d_{31}/d_{15} , d_{22}/d_{15} , d_{33}/d_{15} , and a scale factor).

Single-sarcomere line scan

First, a target sarcomere was selected, and a line was chosen digitally through the A-band to serve as the scan path. A point by point scan was performed along this line. The system collects 512 points per scan; to reduce errors, line scanning was repeated 512 times. Then, a 512-by-512-pixel image was generated. For the next scan, the polarization angle of the excitation light was changed. The polarization-spectrum data were collected in the same way as described in Image Collection and Analysis.

Western blot analysis

Levels of α - and β -myosin expression in the PTU-induced rat cardiomyocytes were evaluated by sodium dodecyl sulfate-polyacrylamide gel electrophoresis analysis, which can separate myosin isoforms in a minigel system. Laemmli sample buffer was used to collect whole cell homogenates from cardiac myocardia treated with PTU for 0, 4, 6, 8, and 10 weeks. Equal amounts of total protein were separated by 4-15% precast protein gels (Bio-Rad Laboratories, Hercules, CA) and transferred onto polyvinylidene difluoride membranes (Bio-Rad Laboratories). α - and β -myosin were probed using a monoclonal anti- α - and anti- β -myosin primary antibody (HPA001239, HPA001349,1:1000 dilution; Sigma-Aldrich), followed by an HRP-labeled anti-rabbit secondary antibody (A16023; Fisher Scientific). Antibodies to α -actin (A2172 (Sigma-Aldrich); A16017, 1:1000 dilution (Thermo Fisher Scientific)) were used in the same Western blot to test for equal loading. After detection of the HRP-conjugated secondary antibodies, the immune complexes were detected by chemiluminescence captured on Biospectrum 500 Imaging System (UVP, Analytik Jena, Upland, CA), and the densitometry of the α - and β -myosin band profiles on the Western blot was performed with ImageJ software (acquired from NIH at http://rsbweb.nih.gov/ij/).

Statistical analysis

In this work, the experimental data are presented as mean ± standard deviation. Statistical analysis was performed with SAS 9.4 software. One-way analysis of variance (ANOVA) tests were used to determine mean separation. Two-sample Student's t-tests were then performed on the average values. p-values of <0.05 were considered to be significant. For each test group, multiple samples (e.g., identical culture chambers) were tested. Before data from different samples in the same test group were merged, Levene's test was used to ensure that equal variance could be assumed.

RESULTS

Polarization spectra of cardiac myosin in ventricles of the five different mammalian species

As shown in Fig. 3 A, the polarization spectra obtained from myosin filaments in mouse or rat ventricles were symmetrical with respect to 90° (consistent with the C6 line profile shown in Fig. 1 Bi), which demonstrated that myosin with C6 crystallographic symmetry dominated in the mouse and rat ventricles. However, the polarization spectra obtained from rabbit, pig, and human ventricles showed significant asymmetry with respect to 90°, demonstrating the existence of considerable C3v symmetric myosin. The values of d_{22}/d_{15} retrieved from rabbit, pig, and human ventricles were also significantly greater than the ones collected from mouse and rat ventricles. Because the difference between C6 symmetry and C3v symmetry depends only on the value of d_{22} / d_{15} , the values of d_{31}/d_{15} and d_{33}/d_{15} are not discussed in this study; these values reflect mainly the arrangement, orientation, and pitch angle of myosin molecules (23). Among all fits in this study, on average, the matching agreement between the data points and the fitting curve was $R^2 > 0.90$.

The polarization spectra and values of d_{22}/d_{15} of myosin filaments as a function of PTU administration period

Without PTU treatment, the polarization spectra of myosin filaments appeared to be a C6 line profile; the retrieved value of d_{22}/d_{15} was 0.02 \pm 0.02, which was consistent with the result shown in Fig. 3 B. However, with the administration of PTU, the polarization spectra of myosin filaments gradually became asymmetrical with respect to 90° and showed a C3v line profile. As the administration period of PTU increased, the polarization spectra approached asymmetry, and the value of d_{22}/d_{15} accordingly increased. For the myosin filaments from 4-, 6-, 8-, and 10-week PTU-treated rat ventricles, the retrieved values of d_{22}/d_{15} were 0.05 ± 0.02 , 0.07 ± 0.03 , 0.11 ± 0.03 , and 0.14 ± 0.04 , respectively.

The results in Fig. 4, A and B indicate that the crystal structure of myosin gradually changed from the original C6 symmetry to C3v symmetry. To further explore the correlation between the transition in polarization spectrum of myosin filaments and the PTU-induced increase in β -myosin content, we performed a Western blot analysis on the rat ventricles tested in Fig. 4 C. In myocardial samples without PTU treatment, α -myosin dominated, and β -myosin was barely detectable. As the PTU administration period increased, the expression of myosin gradually shifted from α - to β -myosin. Applying the quantitative method described in (33,34), the contents of β -myosin were \sim 3, 22, 40, 55, and 85%, respectively, for 0-, 4-, 6-, 8-, and 10-week PTU-treated myocardial samples. Gel lanes, probed with anti- α -actin in Fig. 4 C, indicate that the amounts of protein loading were equal. The Pearson correlation coefficient between the content of β -myosin and the value of d_{22}/d_{15} reached 0.98.

Dynamic transition of the polarization spectrum from a C6 to C3v line profile in NE-treated cardiomyocytes

In the cell-culture experiment, 56 measurement sites were selected for the test and control groups, respectively, as shown in Fig. 5 A using a red box. Because of the death or loss of cells at measurement sites during a 2-day period, we obtained 5 and 34 valid time-dependent observations,

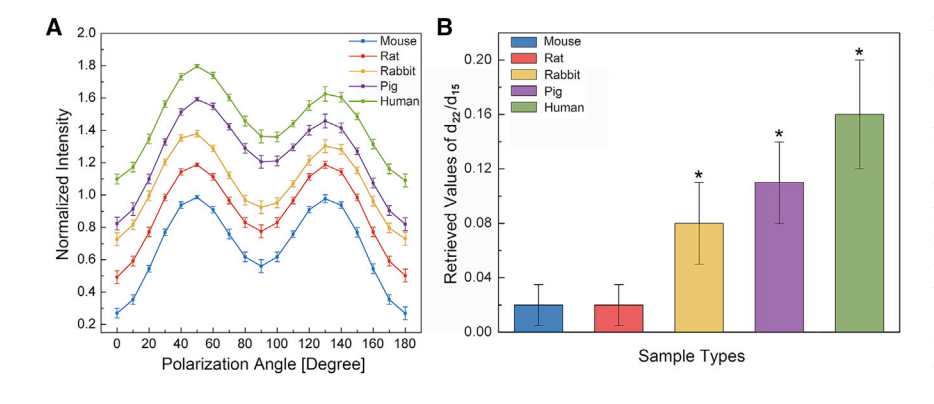


FIGURE 3 (A) Normalized polarization spectra of myosin filaments in ventricles of different mammalian species studied by P-SHG microscopy (for data presentation, the value accumulates 0.2 for each curve). (B) Retrieved values of d_{22}/d_{15} are given: 0.02 ± 0.02 , 0.02 ± 0.02 , $0.08 \pm$ $0.03, 0.11 \pm 0.03, \text{ and } 0.16 \pm 0.04, \text{ respectively,}$ for mouse, rat, rabbit, pig, and human ventricular myocardia. Sample size n = 50 measurements/species: 10-20 sections were arbitrarily selected from the left ventricle free wall; each animal in the test species provided an equal number of sections, with one to four measurements made for each section. One-way ANOVA was followed by Student's *t*-test to compare different groups, *p < 0.05 vs. mouse or rat. No statistical difference was found between animals in a single group. To see this figure in color, go online.

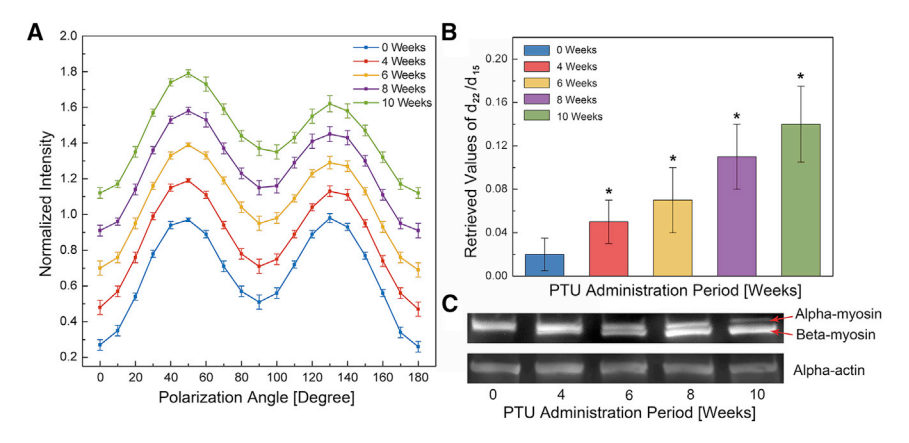


FIGURE 4 (A) Changes in polarization spectra. (B) The corresponding retrieved values of d_{22}/d_{15} of myosin filaments in rat ventricles as a function of PTU administration period are shown (sample size n = 50 measurements/group: 20 sections were arbitrarily selected from left ventricle free wall, and 10 sections were collected per animal in each group; two to four measurements were made for each section). One-way ANOVA was followed by Student's *t*-test to compare groups, *p < 0.05vs. control. No statistical difference was found between animals in a single group. (C) Western blots for 0-, 4-, 6-, 8-, and 10-week PTU-treated rat ventricles are given. Gel lanes were approximately equally loaded as shown by the blot probed with anti- α -actin (as a loading control). To see this figure in color, go online.

respectively, for the test and control groups after the NE administration at 72 h. In the five valid time-dependent observations of the test group, the polarization spectrum of the myosin filaments dynamically transited from C6 to C3v line profile with successive NE administration periods. Fig. 5 B shows the dynamic transition process: the polarization spectra still showed a C6 line type after 24 h of NE administration. However, with the increase in the NE administration period, the polarization spectra gradually shifted to the C3v line profile, which was indicated by the polarization spectra becoming significantly asymmetrical with respect to the 90° at 48 h with continued NE administration and showing more asymmetry at 72 h with continued NE administration. The corresponding retrieved values of d_{22}/d_{15} were 0.03 ± 0.01 , 0.06 ± 0.02 , and 0.08 ± 0.03 at 24, 48, and

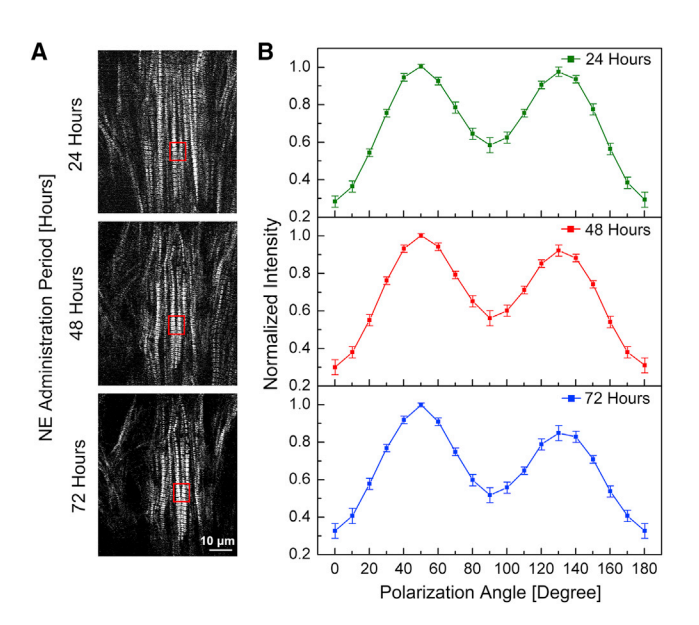


FIGURE 5 (A) Linear-polarized SHG images of cells after NE administration at 24, 48, and 72 h. The red boxes, selected from the same sarcomere group in the same cell, indicate acquisition sites of the polarization spectra. (B) Corresponding polarization spectra collected from the same acquisition sites in cells after NE administration at 24, 48, and 72 h are shown (sample size n = 5). To see this figure in color, go online.

72 h, respectively. Cell morphology measured after the 72-h NE administration showed no significant change. In the 34 valid time-dependent observations of the control group, all polarization spectra of myosin filaments showed a symmetrical C6 line profile. The retrieved values of d_{22}/d_{15} were 0.02 ± 0.01 , 0.03 ± 0.01 , and 0.02 ± 0.01 measured at 24, 48, and 72 h in the control culture, respectively.

The polarization spectra of C3v line-profiled myosin filaments from a single-sarcomere line scan

To locate the structural changes in myosin during the isoform-expression transition from α to β , we performed a single-sarcomere line scan for the 10-week PTU-treated rat ventricles. A total of 100 randomly selected sarcomeres were scanned; half showed a C6 line profile, and half showed a C3v line profile. Fig. 6 B shows the P-SHG imaging results of a typical sarcomere with a C3v line profile. Although the polarization spectrum of this entire sarcomere exhibited a C3v line profile, the polarization spectra of the myosin filaments in different regions of the sarcomere showed two different symmetries: as shown in Fig. 6 C, the polarization spectra of myosin filaments located at the two ends of the A-band (the overlapping regions of myosin backbone and myosin heads) exhibited a C3v line profile, whereas the polarization spectra of myosin filaments located near the M-line remained as the C6 line profile. Moreover, when the overall polarization spectrum of a sarcomere showed a C6 line profile, its polarization spectra in different regions showed uniform symmetry; that is, the polarization spectra of the myosin filaments from the M-line region and from the two ends of the A-band all showed the C6 line profile. These phenomena were supported by the P-SHG imaging results of these 100 sarcomeres.

DISCUSSION

The ratios of the two myosin isoforms in different mammalian myocardia have been extensively studied. It has been

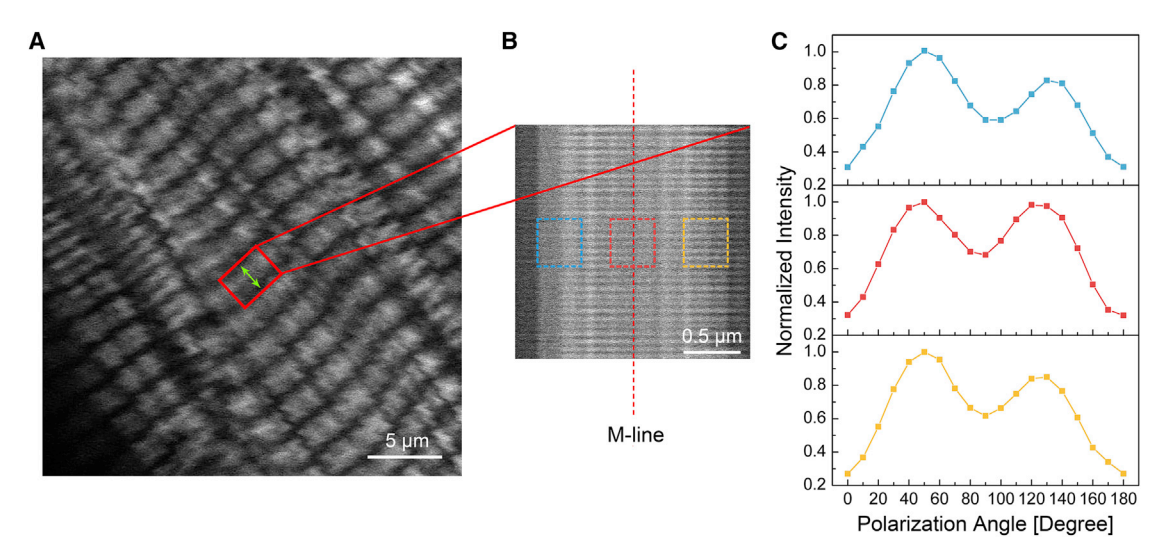


FIGURE 6 (A) Linear-polarized SHG image of the cell whose sarcomere showed a C3v line profile in its polarization spectrum; green arrow indicates line scanning direction. (B) A linear-polarized SHG image of line-scanned sarcomere is given (formed by 512 line scans with the scan direction shown as the green arrow in A). (C) The corresponding polarization spectra collected from the two ends and the M-line areas of the line-scanned sarcomere are shown. Colors of the curves in (C) are consistent with those of the corresponding boxes labeled in (B). To see this figure in color, go online.

demonstrated that α -myosin dominates in month-old rat and mouse ventricles (>90%) (35,36). The ratios of α -/ β myosin in month-old rabbit and adult human ventricles are \sim 1:1 and 1:9, respectively (37,38). As discussed above, the value of d_{22}/d_{15} is the only indicator of myosin symmetry. Thus, for the purpose of analysis, we here declare a threshold value for d_{22}/d_{15} : the myosin in the region of interest is considered to possess C3v symmetry when the value of d_{22}/d_{15} is greater than or equal to 0.08. Using this threshold value of 0.08, measurements 0, 0, 22, and 42 of the 50 selected measurements for mouse, rat, rabbit, and human ventricles showed C3v symmetrical polarization spectra, respectively (Fig. 3). The proportions of myosin with C3v symmetry calculated accordingly agreed well with the reported proportions of β -myosin (<10, <10, 50, and 90%). Furthermore, applying this threshold to the 0-, 4-, 6-, 8-, and 10-week PTU-treated rat ventricles, we found that 0, 8, 18, 29, and 40 of the 50 selected measurements have C3v symmetry. The ratios of α -/ β -myosin obtained from the P-SHG microscopy (0, 16, 36, 58, and 80%) were consistent with those displayed by the Western blot (3, 22, 40, 55, and 85%). Therefore, we suggest that the transition of the polarization spectrum from a C6 to a C3v line profile can be attributed to the expression of β -myosin.

For protein crystals such as myosin and collagen, the intrinsic second harmonic signal lies in the susceptibility of the primary structures of proteins, mainly the amide bonds of polypeptide chains and the peptide bond -CO-HN- between two amino acids (39). However, whether a protein crystal can generate a detectable second harmonic signal depends on its three-dimensional lattice structure, which is determined by the folding, orientation, and symmetry of the protein crystal (40). In the secondary structures of proteins such as α -helices, the susceptibility units are very well ordered, enabling constructive interference of the coherent SHG signal generated by the primary structures. Thus, secondary structures of proteins have an impact on the emission efficiency of an SHG. Further, studies reported in the literature have shown that the symmetry of a protein crystal is decided by tertiary and quaternary structure (41) and, as described previously in this work, can be detected using P-SHG microscopy. Our results demonstrated that the differences in α - and β -myosin studied here were not distinguished by the intensity of SHG signals, which correspond to the protein secondary structure. However, α - and β myosin differences could be distinguished by P-SHG microscopy from the values of nonzero elements in the polarizability tensor, which reflects crystal symmetry at the tertiary and quaternary structural levels.

As shown in Fig. 7, considering a single sarcomeric structure, the M-line area consists of only the myosin coiled tail. The two end sections of the A-band contain both myosin tail and head regions. The single-sarcomere scan results shown in Fig. 6 demonstrate that the polarization-spectrum differences between α - and β -myosin occurred at the two ends of the A-band; these two ends contain both tail and head regions. However, polarization spectra of the M-line region showed that the tail regions located in the myosin filament backbones of α - and β -myosin have the same crystal symmetry. Therefore, our data suggest that differences in the head regions located at the end sections of the A-band gave rise to the difference in the polarization spectra of the two myosin isoforms.

SHG studies of myosin have demonstrated that head regions of the myosin molecule can generate an SHG signal that occupies a considerable proportion of the total SHG

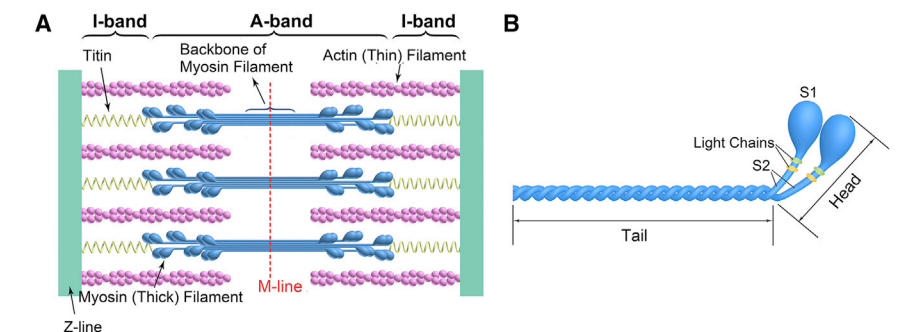


FIGURE 7 (A) Schematic structure of a single sarcomere. (B) The structure of a full-length myosin molecule, which is composed of a tail region (the myosin coiled tail consists of two intertwined α -helices) that lies in the backbone of the myosin filament and a head region (a neck region (S2) connects the two myosin heads (S1) with the myosin tail) that extends from the main myosin filament backbone to attach to an actin filament to form the cross-bridge, is shown. To see this figure in color, go online.

signal produced in muscle (42,43). In addition, it has been determined that the main difference between α - and β -myosin lies in myosin's head region. For example, the differences in the gene sequences of α - and β -myosin are mainly in the gene sequence encoding the myosin head (44). The ATPase activities of a hybrid myosin that consists of the α -myosin tail region and the β -myosin head region are similar to those of β -myosin (15). These studies demonstrate that there are structural differences in head regions between α - and β -myosin, which agrees well with our single-sarcomere scan results (Fig. 6). In addition, other factors, e.g., the differences in the process of assembly of myosin molecules into myosin filaments and the different effects of myosin binding protein-C on α and β myosin, may play a role in leading to the differences in polarization spectrum of α - and β -myosin.

CONCLUSION

Our experimental results show that 1) myosin with C6 symmetry dominated in the small mammalian myocardia, whereas myosin with C3v symmetry dominated in the large mammalian myocardia. It has been widely confirmed that the cardiac myosin in the small and large mammalian myocardia are dominated by the α - and β -isoforms, respectively, and thus, C6 symmetry co-occurs with α -myosin, whereas C3v symmetry occurs with β -myosin; 2) the β -myosin expression increase in PTU-treated rat myocardia was proportionally mirrored by a polarization-spectrum shift from a C6 to a C3v line profile, suggesting that when the ratio of α -/ β -myosin isoforms changes, the ratio of C6/C3v spectra changes proportionally. Hence, there may be a correlation between C6 symmetry and α -myosin and between C3v symmetry and β -myosin; 3) the polarization spectra of myosin filaments, obtained on consecutive culture days from the NE-treated cell culture, gradually shifted from C6 to C3v line profiles. The shift was similar to the chronology reported in the literature for an NE-induced myosin transition from α - to β -isoforms. It is possible that when α -myosin was induced to shift to β -myosin, the myosin structure dynamically changed to C3v symmetry, a further correlation of C6 symmetry to α -myosin and C3v symmetry to β -myosin; 4) correlation of C3v symmetry to β -myosin was observed only at the two end regions of the A-band, in the myosin heads. This is consistent with findings in the literature that the differences between the α - and β -myosin isoforms exist in the head region. All these data can be understood to demonstrate a strong correlation between C6 symmetry and α -myosin and between C3v symmetry and β -myosin. These findings may provide a P-SHG-microscopy-based method for distinguishing α - and β -myosin in living cardiac samples and a method for studying myosinisoform-transfer-related heart disease.

AUTHOR CONTRIBUTIONS

C.Y. performed experiments and data analysis and wrote the initial manuscript draft. X.Z. and Z.W. worked on data analysis and graph generation. T.K.B. focused on biological data analysis. T.Y. modified the imaging system for the study. Z.I.K. provided the human tissue samples and interpreted the relevant data. R.B.R. prepared the samples and revised the manuscript. Y.S. and B.Z.G. acted as the co-PI of the project, proposed the original idea, and revised the manuscript. All authors approved the final version of the

ACKNOWLEDGMENTS

This study was partially supported by National Institutes of Health through SC Centers of Biomedical Research Excellence (COBRE) in the state of South Carolina (P20RR021949 and P20GM130451), R01 funding (R01HL124782 and R01HL144927); National Natural Science Foundation of China (61775148); and the National Science Foundation Established Program to Stimulate Competitve Research (NSF EPSCoR) Program (OIA-1655740).

REFERENCES

- 1. Morkin, E. 1993. Regulation of myosin heavy chain genes in the heart. Circulation. 87:1451-1460.
- 2. Deacon, J. C., M. J. Bloemink, ..., L. A. Leinwand. 2012. Identification of functional differences between recombinant human α and β cardiac myosin motors. Cell. Mol. Life Sci. 69:2261-2277.
- 3. Lompré, A. M., B. Nadal-Ginard, and V. Mahdavi. 1984. Expression of the cardiac ventricular alpha- and beta-myosin heavy chain genes is developmentally and hormonally regulated. J. Biol. Chem. 259:6437-
- 4. Fitzsimons, D. P., J. R. Patel, and R. L. Moss. 1998. Role of myosin heavy chain composition in kinetics of force development and relaxation in rat myocardium. J. Physiol. 513:171-183.

- Herron, T. J., and K. S. McDonald. 2002. Small amounts of alphamyosin heavy chain isoform expression significantly increase power output of rat cardiac myocyte fragments. Circ. Res. 90:1150–1152.
- Everett, A. W., A. M. Sinha, ..., R. Zak. 1984. Regulation of myosin synthesis by thyroid hormone: relative change in the alpha- and betamyosin heavy chain mRNA levels in rabbit heart. *Biochemistry*. 23:1596–1599.
- Stelzer, J. E., S. L. Brickson, ..., R. L. Moss. 2007. Role of myosin heavy chain composition in the stretch activation response of rat myocardium. *J. Physiol.* 579:161–173.
- Krenz, M., and J. Robbins. 2004. Impact of beta-myosin heavy chain expression on cardiac function during stress. J. Am. Coll. Cardiol. 44:2390–2397.
- Kurabayashi, M., H. Tsuchimochi, ..., Y. Yazaki. 1988. Molecular cloning and characterization of human cardiac alpha- and beta-form myosin heavy chain complementary DNA clones. Regulation of expression during development and pressure overload in human atrium. J. Clin. Invest. 82:524–531.
- Locher, M. R., M. V. Razumova, ..., R. L. Moss. 2011. Effects of low-level α-myosin heavy chain expression on contractile kinetics in porcine myocardium. Am. J. Physiol. Heart Circ. Physiol. 300:H869–H878
- Lowes, B. D., W. Minobe, ..., M. R. Bristow. 1997. Changes in gene expression in the intact human heart. Downregulation of alpha-myosin heavy chain in hypertrophied, failing ventricular myocardium. *J. Clin. Invest.* 100:2315–2324.
- Mercadier, J. J., D. de la Bastie, ..., K. Schwartz. 1987. Alpha-myosin heavy chain isoform and atrial size in patients with various types of mitral valve dysfunction: a quantitative study. *J. Am. Coll. Cardiol*. 9:1024–1030.
- Fogle, R. L., C. J. Lynch, ..., T. C. Vary. 2010. Impact of chronic alcohol ingestion on cardiac muscle protein expression. *Alcohol. Clin. Exp. Res.* 34:1226–1234.
- McNally, E. M., R. Kraft, ..., L. A. Leinwand. 1989. Full-length rat alpha and beta cardiac myosin heavy chain sequences. Comparisons suggest a molecular basis for functional differences. *J. Mol. Biol.* 210:665–671.
- Krenz, M., S. Sadayappan, ..., J. Robbins. 2007. Distribution and structure-function relationship of myosin heavy chain isoforms in the adult mouse heart. J. Biol. Chem. 282:24057–24064.
- Alpert, N. R., C. Brosseau, ..., D. M. Warshaw. 2002. Molecular mechanics of mouse cardiac myosin isoforms. Am. J. Physiol. Heart Circ. Physiol. 283:H1446–H1454.
- Piao, S., F. Yu, ..., J. A. Bauer. 2003. A simplified method for identification of human cardiac myosin heavy-chain isoforms. *Biotechnol. Appl. Biochem.* 37:27–30.
- Talmadge, R. J., and R. R. Roy. 1993. Electrophoretic separation of rat skeletal muscle myosin heavy-chain isoforms. *J. Appl. Physiol.* 75:2337–2340.
- Helmke, S. M., C. Y. Yen, ..., M. B. Perryman. 2004. Simultaneous quantification of human cardiac alpha- and beta-myosin heavy chain proteins by MALDI-TOF mass spectrometry. *Anal. Chem.* 76:1683– 1689.
- Campagnola, P. J., and L. M. Loew. 2003. Second-harmonic imaging microscopy for visualizing biomolecular arrays in cells, tissues and organisms. *Nat. Biotechnol.* 21:1356–1360.
- Odin, C., T. Guilbert, ..., Y. Le Grand. 2008. Collagen and myosin characterization by orientation field second harmonic microscopy. Opt. Express. 16:16151–16165.
- Psilodimitrakopoulos, S., P. Loza-Alvarez, and D. Artigas. 2014. Fast monitoring of in-vivo conformational changes in myosin using single scan polarization-SHG microscopy. *Biomed. Opt. Express.* 5:4362– 4373.
- Tiaho, F., G. Recher, and D. Rouède. 2007. Estimation of helical angles of myosin and collagen by second harmonic generation imaging microscopy. Opt. Express. 15:12286–12295.

- Butcher, P. N., and D. Cotter. 2003. The Elements of Nonlinear Optics. Cambridge University Press, Cambridge, UK.
- Ambekar, R., T. Y. Lau, ..., K. C. Toussaint, Jr. 2012. Quantifying collagen structure in breast biopsies using second-harmonic generation imaging. *Biomed. Opt. Express*. 3:2021–2035.
- Shao, Y. H., H. H. Liu, ..., B. Gao. 2011. 3D myofibril imaging in live cardiomyocytes via hybrid SHG-TPEF microscopy. *Proc. SPIE*. 7903:79030F.
- Giger, J., A. X. Qin, ..., F. Haddad. 2007. Activity of the beta-myosin heavy chain antisense promoter responds to diabetes and hypothyroidism. *Am. J. Physiol. Heart Circ. Physiol.* 292:H3065–H3071.
- Wright, C. E., F. Haddad, ..., K. M. Baldwin. 1999. In vivo regulation of beta-MHC gene in rodent heart: role of T3 and evidence for an upstream enhancer. Am. J. Physiol. 276:C883–C891.
- Ma, Z., R. K. Pirlo, ..., B. Z. Gao. 2011. Laser-guidance-based cell deposition microscope for heterotypic single-cell micropatterning. *Bio-fabrication*. 3:034107–034116.
- Waspe, L. E., C. P. Ordahl, and P. C. Simpson. 1990. The cardiac betamyosin heavy chain isogene is induced selectively in alpha 1-adrenergic receptor-stimulated hypertrophy of cultured rat heart myocytes. *J. Clin. Invest.* 85:1206–1214.
- 31. Simpson, P. 1985. Stimulation of hypertrophy of cultured neonatal rat heart cells through an alpha 1-adrenergic receptor and induction of beating through an alpha 1- and beta 1-adrenergic receptor interaction. Evidence for independent regulation of growth and beating. Circ. Res. 56:884–894.
- 32. Simpson, P. 1983. Norepinephrine-stimulated hypertrophy of cultured rat myocardial cells is an alpha 1 adrenergic response. *J. Clin. Invest.* 72:732–738.
- Cagnan, I., E. Cosgun, ..., A. Gunel-Ozcan. 2019. PKNOX2 expression and regulation in the bone marrow mesenchymal stem cells of Fanconi anemia patients and healthy donors. *Mol. Biol. Rep.* 46:669–678.
- Davarinejad, H. 2017. Quantifications of Western Blots with ImageJ. http://www.yorku.ca/yisheng/Internal/Protocols/ImageJ.pdf.
- Hydock, D. S., K. Y. Wonders, ..., R. Hayward. 2009. Voluntary wheel running in rats receiving doxorubicin: effects on running activity and cardiac myosin heavy chain. *Anticancer Res.* 29:4401–4407.
- Hoh, J. F., P. A. McGrath, and P. T. Hale. 1978. Electrophoretic analysis
 of multiple forms of rat cardiac myosin: effects of hypophysectomy
 and thyroxine replacement. J. Mol. Cell. Cardiol. 10:1053–1076.
- Miyata, S., W. Minobe, ..., L. A. Leinwand. 2000. Myosin heavy chain isoform expression in the failing and nonfailing human heart. *Circ. Res.* 86:386–390.
- Gupta, M. P. 2007. Factors controlling cardiac myosin-isoform shift during hypertrophy and heart failure. J. Mol. Cell. Cardiol. 43:388–403.
- Conboy, J. C., and M. A. Kriech. 2003. Measuring melittin binding to planar supported lipid bilayer by chiral second harmonic generation. *Anal. Chim. Acta.* 496:143–153.
- Haupert, L. M., E. L. DeWalt, and G. J. Simpson. 2012. Modeling the SHG activities of diverse protein crystals. *Acta Crystallogr. D Biol.* Crystallogr. 68:1513–1521.
- Myers-Turnbull, D., S. E. Bliven, ..., A. Prlić. 2014. Systematic detection of internal symmetry in proteins using CE-Symm. J. Mol. Biol. 426:2255–2268.
- Samim, M., N. Prent, ..., V. Barzda. 2014. Second harmonic generation polarization properties of myofilaments. J. Biomed. Opt. 19:056005.
- Nucciotti, V., C. Stringari, ..., F. S. Pavone. 2010. Probing myosin structural conformation in vivo by second-harmonic generation microscopy. *Proc. Natl. Acad. Sci. USA*. 107:7763–7768.
- 44. Matsuoka, R., K. W. Beisel, ..., A. Takao. 1991. Complete sequence of human cardiac alpha-myosin heavy chain gene and amino acid comparison to other myosins based on structural and functional differences. *Am. J. Med. Genet.* 41:537–547.